Supporting Information

Horn and Nicoll 10.1073/pnas.1719523115

SI Materials and Methods

Details of Mouse Transgenic Lines. To express ChR2 in PV-positive interneurons, PV-IRES-Cre mice (Jackson Laboratory Strain 008069) were bred with Ai32 mice, a Cre-dependent ChR2 line (Jackson Laboratory Strain 012569). To express ChR2 in SOM-positive interneurons, SOM-IRES-Cre mice (Jackson Laboratory Strain 013044) were bred with Ai32 mice. Mice that were either heterozygous or homozygous for each gene were used for organotypic slice culture dissection. PV-IRES-Cre and SOM-IRES-Cre mice were a gift of V. S. Sohal, University of California, San Francisco, and Ai32 mice were a gift of Z. A. Knight, University of California, San Francisco. Animals were housed according to the Institutional Animal Care and Use Committee guidelines at the University of California, San Francisco.

Experimental Constructs. For CRISPR constructs, the following gRNA targeting sequences were used (5′ to 3′): Nav1.1, 1.2, and 1.3: TCCACTCCCCACACAGCACG; Nav1.6: GCTGCTGCAGAATGAGAAGA; GluN1 gRNA #1 AACCAGGCCAATAAGCGACA (validated in ref. 25): GluN1 gRNA #2: AACCAGCCCACACCATGCCT (validated in ref. 24), GluN1 gRNA #3 ACTAGGATAGCGTAGACCTG (validated in ref. 25). The gRNA sequences were ligated into pX458 to coexpress the human codon-optimized Cas9 as previously described (25). To target sodium channels, we triple-coated gold particles with pX458 expressing gRNA targeting Nav1.1, 1.2, 1.3, pX458 expressing gRNA targeting Nav1.6, and pCAGGS-mCherry expressing plasmid to aid identification of transfected cells. To target GluN1, we cocoated the gold particles with either a pX458 plasmid expressing gRNA #1, gRNA #2, or gRNA #3, along with pCAGGS-mCherry. GluN1 N616R was mutated from the GluN1-1a splice variant and expressed in a pCAGGS expression plasmid (pCAG-GluN1 N616R-IRES-mCherry). Gephyrin miR targeting sequence was AACAGGGAATGAGCTACTAAA, validated in ref. 30. Collybistin shRNA targeting sequence was AATCCGGAGAGACATCCTATA, validated in refs. 50 and 51 and in Fig. S3*A*. NLGN2 miR targeting sequence was ATGGAGCAAGTTCAACAGCAA, validated in ref. 30. NLGN3 miR targeting sequence was GCAGCGTTCTTGCAAGTTATG, validated in ref. 52. The NLGN3 overexpression construct was expressed in a pCAGGS expression construct containing IRES mCherry and was based on human NLGN3 (NCBI accession no. BC051715).

Details of Slice Culture and Biolistic Transfection. Hippocampal organotypic slice cultures were prepared from postnatal day 6–8 mice as described previously (53). All experiments were performed in accordance with established protocols approved by the University of California, San Francisco Institutional Animal Care and Use Committee. Sparse biolistic transfections of organotypic slice cultures were performed as previously described (54). Briefly, 50 μg each of plasmid DNA was coated on 1-μm-diameter gold particles in 0.5 mM spermidine, precipitated with 0.1 mM $CaCl_2$, and washed four times in pure ethanol. The gold particles were coated onto PVC tubing, dried using ultra-pure N_2 gas, and stored at 4 °C in desiccant. DNA-coated gold particles were delivered with a Helios Gene Gun (Bio-Rad). Slices were maintained at 34 °C with media changes three times a week. All constructs were transfected on day 1 in vitro. Construct expression was confirmed by GFP and/or mCherry fluorescence. For the D-APV, MK-801, nifedipine, and SNX-482 experiments, slices were incubated in the drug from the time of transfection to the time of recording. SNX-482 was obtained from Peptides International, and BSA (0.1 mg/mL) was added to the media to minimize nonspecific peptide binding.

Details of Electrophysiological Recording. Recordings were performed at 14–21DIV. Dual whole-cell recordings in area CA1 were done by simultaneously recording responses from a fluorescent transfected neuron and a neighboring untransfected control neuron. IPSCs were recorded at 0 mV. For photostimulation, blue light was emitted from a Prizmatix UHP-LCC LED at 10-s ISIs. Intensity (0.05–1 mW) and duration (~5 ms) of light pulses were adjusted to produce reliable IPSCs of 100–1,000 pA. We performed all recordings on an Olympus BX51WI microscope, using an Olympus ACROPLAN 63×/0.90 W objective.

NMDAR currents were evoked with a bipolar electrode placed in stratum radiutum and were measured at +40 mV in two different ways: (*i*) after the after wash-on of picrotoxin (0.1 mM) and bicuculline (0.01 mM), 150 ms after the stimulation, to ensure that any currents recorded were purely NMDAR-mediated (as in Fig. S3*G*) or (*ii*) with the additional presence of NBQX (50 μM), measuring amplitude at the initial peak (as in Fig. S3*A*). Twenty to 50 sweeps were averaged per pair. Typically each pair of neurons is from a separate slice, whereas on rare occasions two pairs may come from one slice. For all paired recordings, the number of experiments (*n*) reported in the figure legends refers to the number of pairs. CA1 PNs were identified by morphology and location. Transfection under these conditions was sparse, and slices in which possible interneurons were also transfected in the same slice as a CA1 PN were thrown out. To ensure stable recording, membrane holding current, input resistance, and pipette series resistance were monitored throughout recording. All recordings were made at 20–25 °C using glass patch electrodes filled with an internal solution. Cesium-based internal solution was used for the majority of experiments and consisted of 135 mM $CsMeSO_3$, 8 mM NaCl, 10 mM Hepes, 0.3 mM EGTA, 4 mM Mg-ATP, 0.3 mM Na-GTP, 5 mM QX-314, and 0.1 mM spermine. Potassium-based internal solution was used to validate the ΔNav construct and consisted of 135 mM $KMeSO_4$, 10 mM NaCl, 2 mM $MgCl_2$, 1 mM EGTA, 10 mM Hepes, 14 mM phosphocreatine, 4 mM Mg-ATP, and 0.3 mM Na-GTP. External solution contained 119 mM NaCl, 2.5 mM KCl, 4 mM $MgSO_4$, 4 mM $CaCl_2$, 1 mM NaH_2PO_4, 26.2 mM $NaHCO_3$, and 11 mM glucose and was bubbled continuously with 95% O_2 and 5% CO_2. For the ΔNav experiments, $KMeSO_4$-based internal was used to validate the construct, pulsing increasing amounts of current until the ΔNav cell either fired residual action potentials (Fig. S2*A*) or failed to fire action potentials even with currents sufficient to elicit trains of action potentials in control cells (Fig. 3*A*). We initially recorded some PV-IPSCs and SOM-IPSCs using the $KMeSO_4$-based internal. After ensuring our ΔNav technique reliably eliminated or significantly reduced action potentials, we switched to using a cesium-based internal. We found no difference between these conditions and therefore combined the datasets.

PPRs were examined using optogenetically evoked IPSCs at 50-, 100-, 200-, 400-, and 800-ms intervals. Six stimuli were averaged per interval for each cell. Transfected and control neurons were recorded serially, adjusting the stimulus intensity for each neuron so that the first pulse produced IPSCs with ~200-pA peak amplitudes. Control neurons and transfected neurons were recorded from the same slice to control for interslice variation, moving to a new field of illumination in CA1 for the second recorded neuron, and varying whether the transfected or untransfected neuron was recorded from first. To measure the height of the second IPSC in

cases where the first IPSC was overlapping with the second, we subtracted the contribution from the first IPSC, measuring from the point on the *y* axis at which second IPSC began to its peak.

Dissociated Neuronal Preparation, Lentivirus Production, and Real-Time PCR for Fig. S1. HEK293T cells were cotransfected with psPAX2, pVSV-G, and collybistin shRNA viral construct using FuGENE HD (Promega). Supernatant was collected 40 h later, filtered, and concentrated using PEG-it Virus Precipitation Solution (System Biosciences). Resulting pellet was resuspended in Opti-mem, flash-frozen, and stored at –80 °C.

Primary rat hippocampal dissociated neurons were prepared at embryonic day18.5 and infected with lentivirus expressing a collybistin shRNA or control GFP construct at DIV4–7. Neurons were harvested at DIV17–18 by lysis and reverse-transcribed to synthesize cDNA using a Power SYBR Green Cells-to-CT kit (Life Technologies). Amplification of cDNA by real-time PCR was quantified using SYBR Green with the following primers: (fwd) TGCAAGAAGGACCTAATCCG, (rev) TCTCTT CTCTGAAAGCTCTAAGC.

CV Analysis. CV analysis can be used to determine whether the locus of the decrease in PV- and SOM-IPSCs is due to a change in quantal size (q) or quantal content ($N \times P_r$). To perform this analysis, we calculated the CV^{-2}, defined as the (M^2/SD^2), where M is the mean IPSC amplitude and SD is the SD for a set of successive sweeps. We calculated the CV^{-2} for the experimental and control cell and plotted this ratio ($CV^{-2}_{Expt}/CV^{-2}_{Ctl}$) against the ratio in mean amplitude (M_{Expt}/M_{Ctl}). Each of the gray circles in Figs. 3*F* and 4*I* represent a single pair of neurons. If these data points fall on the y = 1 line, the change in IPSC amplitude represents a change in quantal size, while if the data points fall on the identity line (gray dashed line) the change in IPSC amplitude represents a change in quantal content. This relies on the fact that changes in quantal size change both the mean IPSC and the variance such that the normalized ratio of CV^{-2} remains constant. In contrast, changes in quantal content will cause proportional changes of equal magnitude in CV^{-2}. See refs. 19 and 55 for a more detailed description of this technique.

Details for Statistical Analysis. All paired whole-cell data were analyzed using a two-tailed Wilcoxon matched-pairs signed rank test. For comparisons of nonpaired data including intrinsic excitability properties (Fig. S2 *B–D*), paired-pulse depression (Figs. S2*E* and S3*F*), and Fig. S3*B*, a Mann–Whitney *U* test was used. Outliers in IPSC data were removed using a ROUT test, Q = 5% on the $\log_{10}$ transfected–control data, on all paired IPSC datasets (3 out of 403 pairs were removed). For measuring rise time and action potential height, the start of the action potential was defined as the point at which the action potential reached 10% of its maximum slope. Data analysis was carried out in Igor Pro (Wavemetrics), GraphPad Prism (GraphPad Software), and Excel (Microsoft).

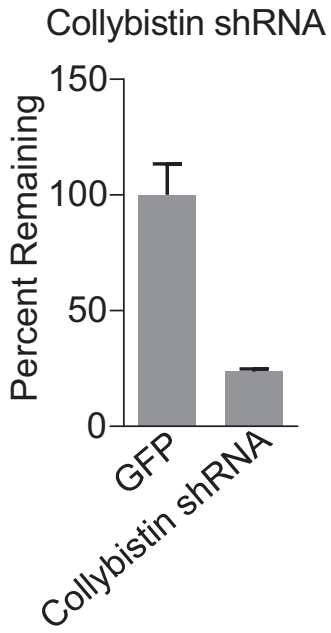

Fig. S1. Quantification of collybistin shRNA efficiency. Graph shows mean ± SEM of collybistin mRNA remaining following treatment of dissociated hippocampal neurons with a virus expressing collybistin shRNA as assessed by real-time quantitative PCR, normalized to control GFP transduction (n = 2 technical replicates).

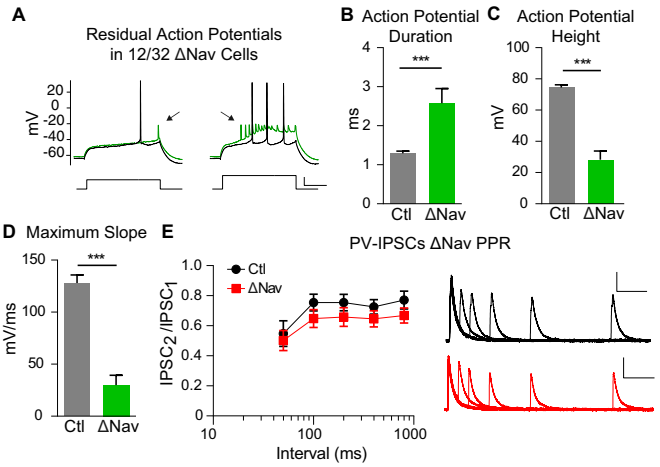

Fig. S2. Validation of ΔNav experimental construct and PPR analysis on PV-IPSCs. (*A*) Sample traces from neurons expressing ΔNav (green traces), or neighboring control neurons (black traces), showing a show typical transfected cell with residual action potentials (see arrows), as in 12 of 32 cells. (Scale bars: 100 pA and 100 ms.) (*B–D*) Summary plots show mean ± SEM on residual action potentials, showing increased rise time (*B*), decreased action potential height (*C*), and decreased maximum slope (*D*) compared with control cell action potentials ($n = 12$ transfected cells, $n = 23$ control cells). ***$P < 0.001$. (*E*) PPRs of PV-IPSCs ($IPSC_2/IPSC_1$) recorded as a function of the ISI in milliseconds. Summary plot shows mean PPR ± SEM for each interval, in ΔNav and control cells. To the right are representative traces of PV-IPSCs for both control (black) and ΔNav (red) cells, overlaid to show all intervals tested (50, 100, 200, 400, and 800 ms). (Scale bars: 100 pA and 150 ms.) At no interval was there a statistically significant difference between the PPR in ΔNav and control cells. $n = 9$ transfected cells, and $n = 9$ control cells.

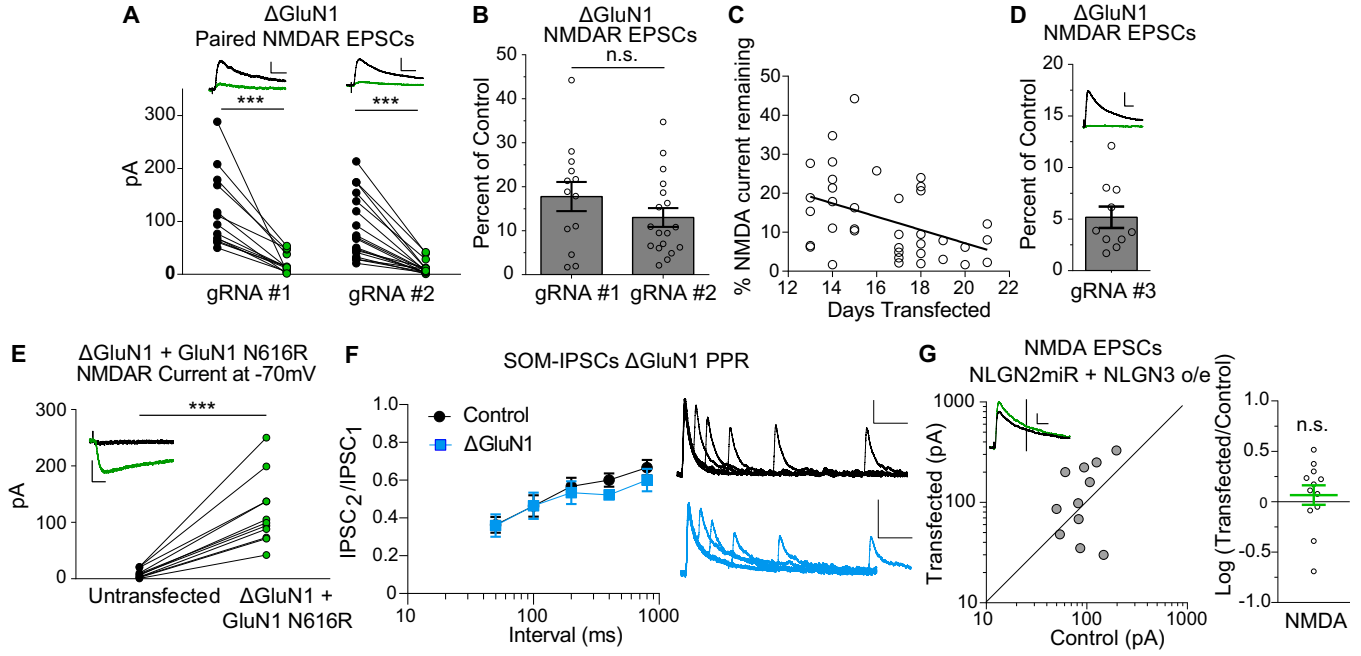

Fig. S3. Effects of ΔGluN1 and GluN1 N616R on NMDAR currents and PPR analysis on SOM-IPSCs. (*A*) Paired data showing effects of GluN1 gRNA #1 and GluN1 gRNA #2 on NMDAR currents (gRNA #1, $n = 13$; gRNA #2, $n = 18$). (Scale bars: 50 pA and 50 ms.) (*B*) Summary plot showing NMDAR currents as a percent of control mean ± SEM. (*C*) Plot showing trend of further reductions of NMDAR currents with more days transfected. (*D*) Summary plot showing NMDAR currents remaining after transfection with intronic targeting GluN1 gRNA #3 (mean ± SEM, $n = 10$). (Scale bars: 50 pA and 50 ms.) (*E*) Paired data showing the effect of coexpressing ΔGluN1 (gRNA #3) with GluN1 N616R on NMDAR currents recorded at −70 mV ($P < 0.001$, $n = 11$). (Scale bars: 50 pA and 50 ms.) (*F*) PPRs of SOM-IPSCs ($IPSC_2/IPSC_1$) recorded as a function of the ISI in milliseconds. Summary plot shows mean PPR ± SEM for each interval, in ΔGluN1 and control cells. To the right are representative traces of SOM-IPSCs for both control (black) and Δ GluN1 (blue) cells, overlaid to show all intervals tested (50, 100, 200, 400, and 800 ms). (Scale bars: 100 pA and 150 ms.) At no interval was there a statistically significant difference between the PPR in ΔGluN1 and control cells. $n = 8$ transfected cells and $n = 8$ control cells. (*G*) Scatter plot shows amplitudes of electrically evoked NMDAR-mediated current recorded from pairs of NLGN2miR + NLGN3 o/e transfected and control cells at ∼18DIV (transfected ∼2.5 wk) in PV:ChR2 mice, in the presence of bicuculin and picrotoxin, amplitude taken at 150 ms after stimulation (indicated by solid black line in sample trace) to eliminate contribution from AMPAR-mediated currents. Summary plot showing IPSCs as a $\log_{10}$ of the ratio between transfected and control neurons, mean ± SEM ($P > 0.05$, $n = 11$). Black sample traces are control and green traces are transfected cells. (Scale bars: 50 pA and 50 ms.) ***$P < 0.001$.

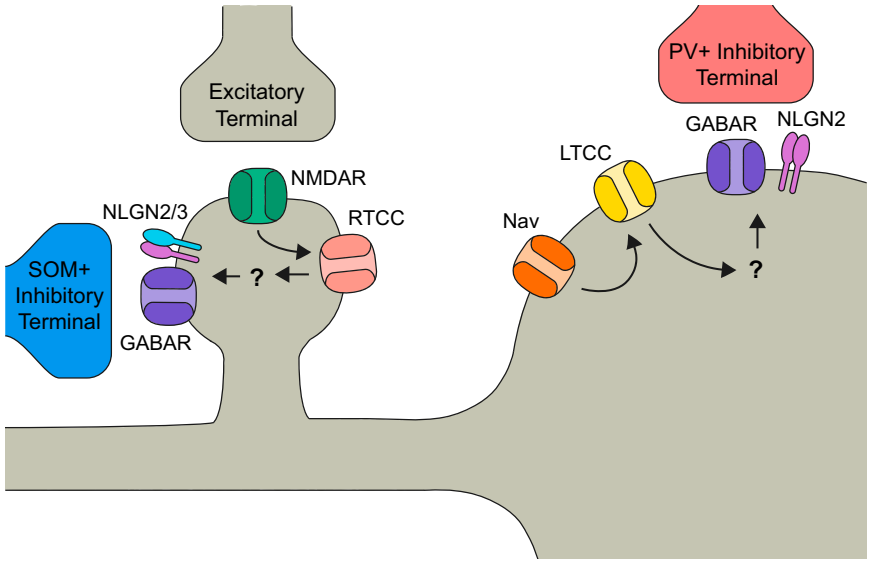

Fig. S4. Model summarizing results: PV-IPSCs are regulated by sodium channel (Nav). Mediated action potentials, a process dependent on LTCC. SOM-IPSCs are regulated by NMDARs, a process dependent on RTCC. PV-IPSCs require neuroligin-2 (NLGN2), while SOM-IPSCs require both NLGN2 and neuroligin-3 (NLGN3). Not pictured are NLGN2/2 or NLGN3/3 homomers, which are also likely present at synapses formed by SOM-expressing inhibitory neurons.